

Direct seismic energy modeling and application to the 1979 Imperial Valley earthquake

Pascal Favreau and Ralph J. Archuleta

Institute for Crustal Studies, University of California at Santa Barbara, Santa Barbara, California, USA

Received 24 July 2002; accepted 14 January 2002; published 4 March 2003.

[1] The seismic energy associated with an earthquake has two representations: the work of the seismic waves done against a distant surface or a fault representation. For a fault subject to slip-weakening friction, the energy density is the difference between an elastostatic work and a work density spent in fracture and relaxation. We apply this to a dynamic simulation of the 1979 Imperial Valley earthquake, whose initial conditions are inspired by previous kinematic studies. A large area of the fault has a negative energy density, and the emission of energy is roughly confined to small parts of the fault with large positive energy density. We compute the work of the seismic waves against the surface of a sphere enclosing the source, and we find the same amount of energy. We produce a map of energy directivity that shows that 40% of the energy passes through only 6.5% of the sphere. *INDEX TERMS*: 7209 Seismology: Earthquake dynamics and mechanics; 7260 Seismology: Theory and modeling; 7299 Seismology: General or miscellaneous. **Citation**: Favreau, P., and R. J. Archuleta, Direct seismic energy modeling and application to the 1979 Imperial Valley earthquake, *Geophys. Res. Lett.*, 30(5), 1198, doi:10.1029/2002GL015968, 2003.

1. Introduction

[2] Seismic energy is one of the global quantities that defines the size of the earthquakes [Gutenberg and Richter, 1942]. The first one, although second historically, is the seismic moment [Aki, 1966]. The second is the seismic energy that relates to the dynamics of the rupture process. However, seismic energy is more difficult to estimate than seismic moment [see Kanamori et al., 1993; Choy and Boatwright, 1995]. This limits our general knowledge on the mechanical process of the rupture: no reliable catalog of seismic energy is available today and the experimental relation between static and dynamic properties can not be fully determined. Here, we propose to investigate these questions in the light of the direct modeling of the dynamic rupture process. This is possible because the fault kinematics have been determined for several earthquakes. This information provides a set of reasonable and reliable initial conditions for the dynamic models [see Peyrat et al., 2001].

2. The Seismic Energy

[3] To be universal, the seismic energy must be a unique quantity that depends only on the dynamics of the source. Let us consider any source process, lasting a finite amount of time and occurring on a fault plane defined by the surface

Σ . We define a distant surface of observation S surrounding the source process and V the volume embedded between S and Σ . As in Kostrov [1974], we define the work done by the seismic waves against S :

$$W_q^S = \int_S w_q^S dS; \quad w_q^S = - \int_{t^0}^{t^1} \dot{u}_i (\sigma_{ij} - \sigma_{ij}^0) n_j dt$$

where u_i is the displacement field, σ_{ij} is the stress tensor and n_j is the outer normal of S . Superscripts 0 and 1 correspond to the values at the times t^0 and t^1 . The initial displacement field u_i^0 is set to zero.

[4] It would be enough that t^0 and t^1 be the beginning and the end of each record on the surface S ; however, to simplify we consider that t^0 is the time of beginning of the rupture and t^1 is the time for the volume V to reach a state of rest. Depending on S , reflections and scattering in the crust, t^1 can be much larger than the duration of the source itself. If the volume V is a linear elastic solid and if the slipping process on Σ is not singular, that is, if the stresses and the slip velocities remain continuous in time and space, we have:

$$W_q^S = E_q + W_e^S$$

$$E_q = \int_{\Sigma} \left(-\frac{1}{2} \delta u_i^1 (\sigma_{ij}^1 - \sigma_{ij}^0) + \int_{t^0}^{t^1} \delta u_i \dot{\sigma}_{ij} dt \right) n_j' d\Sigma \quad (1)$$

$$W_e^S = \int_S w_e^S dS; \quad w_e^S = -\frac{1}{2} u_i^1 (\sigma_{ij}^1 - \sigma_{ij}^0) n_j$$

where δu_i is the displacement discontinuity on Σ that is defined accordingly to the normal n_j' of Σ . E_q is the far field seismic energy and W_e^S is the elastostatic work done on the surface S . Some comments must be made about relation (1). Firstly, W_q^S is not independent of the surface S because it contains the elastostatic work W_e^S which involves S . However, in the far-field when the characteristic radius R of S is much larger than the source dimension L , this work becomes negligible. We have $\lim_{R/L \rightarrow \infty} W_q^S = E_q$. Although E_q is equal to W_q^S in the far-field only, it is uniquely determined by the rupture process. Secondly, a major contribution to E_q , is the release of volumetric, prestress-free, strain energy by the crust which is mapped on the fault by the elastostatic work $W_e^{\Sigma} = \int_{\Sigma} -\frac{1}{2} \delta u_i^1 (\sigma_{ij}^1 - \sigma_{ij}^0) n_j' d\Sigma$. This surface representation is deduced by Stoke's theorem. For a straight fault that slips without opening at constant rake we simply have:

$$W_e^{\Sigma} = \int_{\Sigma} w_e^{\Sigma} d\Sigma; \quad w_e^{\Sigma} = -\frac{1}{2} \delta u^1 (\tau^1 - \tau^0) \quad (2)$$

where δu and τ denote the slip and the shear stress parallel to the slip on the fault, respectively. Thirdly, unlike Kostrov

[1974], we have not considered an ideally brittle material (abrupt stress drop model) but a model regularized by a cohesive zone. Therefore, the fracture energy is contained in the time integral of the product of the stress time derivative and the dislocation. To demonstrate this in the simplest case, let us limit our problem to a straight fault that slips (without back-slip) at constant rake. Let us define the shear resistance of the fault by a slip-weakening friction law

$$\tau \leq \tau^y \text{ if } \delta\dot{u} = 0 \text{ and } \tau = \tau^y \text{ if } \delta\dot{u} > 0 \quad (3)$$

$$\tau^y(\delta u) = \tau_s + (\tau_d - \tau_s) \inf(\delta u / D_c, 1) \quad (4)$$

where $\delta\dot{u}$ denotes the fault slip velocity, and τ^y denotes the slip-dependent yield resistance of the fault. τ_s , τ_d and D_c are the parameters associated with the fault resistance: the maximal resistance (“static”), the residual resistance (“dynamic”), and the critical slip needed to achieve the stress breakdown, respectively.

[5] By assuming the formulation (3) and (4), one finds that, in (1), $\int_{\Sigma} \int_{\rho} \delta u_i \delta \dot{t} n'_j d\Sigma = -W_f^{\Sigma} - W_r^{\Sigma}$ where:

$$W_f^{\Sigma} = \int_{\Sigma} w_f^{\Sigma} d\Sigma; \quad w_f^{\Sigma} = \frac{1}{2} (\tau_s - \tau^y(\delta u^1)) \inf(\delta u^1, D_c)$$

$$W_r^{\Sigma} = \int_{\Sigma} w_r^{\Sigma} d\Sigma; \quad w_r^{\Sigma} = \delta u^1 (\tau^y(\delta u^1) - \tau^1)$$

w_f^{Σ} is the fracture work spent in the breakdown at the rupture front and w_r^{Σ} is the work done by the stress relaxation on the fault after the arrest of the slip [see *Madariaga*, 1976]. Our expressions for w_f^{Σ} and w_r^{Σ} are valid for any value of the final slip δu^1 . If the final slip δu^1 exceeds the critical slip D_c we have simplifications: $w_f^{\Sigma} = \frac{1}{2}(\tau_s - \tau_d)D_c$ (all the fracture work is spent) and $w_r^{\Sigma} = \delta u^1 (\tau_d - \tau^1)$. To conclude, the seismic energy can be mapped on the fault as $E_q = \int_{\Sigma} e_q^{\Sigma} d\Sigma$ where $e_q^{\Sigma} = w_e^{\Sigma} - w_f^{\Sigma} - w_r^{\Sigma}$ is the energy density that includes the work density contributions of elastic, fracture and relaxation. This decomposition, however not unique, is an optimal fault mapping that shows source and dissipation and removes the initial state. In Figure 1, we give a graphical representation of these contribution to e_q^{Σ} for the case $\delta u^1 > D_c$. Depending on the different contributions, we expect that the density e_q^{Σ} can be locally negative, but its integral on the fault E_q must be positive.

3. A Dynamic Model for the 1979 Imperial Valley Earthquake

[6] To produce a map of seismic energy density on the fault, we construct an heterogeneous spontaneous rupture model for the strike-slip 1979 Imperial Valley earthquake with the failure criterion defined by (3) and (4). We use a finite-difference method on a velocity-stress staggered grid. Time and space derivatives in the interior are respectively evaluated at 2nd and 8th order. At the boundaries, the order in space decreases progressively in an absorbing perfectly-matched layer. The fault slip is introduced as a stress glut [see *Andrews*, 1999] and, to remain 2nd order in time, the slip is evaluated implicitly. For the crustal heterogeneity, the effective elastic parameters are averaged in the manner of *Moczo et al.* [2003].

[7] Based on the inversion of the strong ground motion, the kinematic fault model of *Archuleta* [1984], exhibits an heterogeneous slip and a rupture velocity that varies

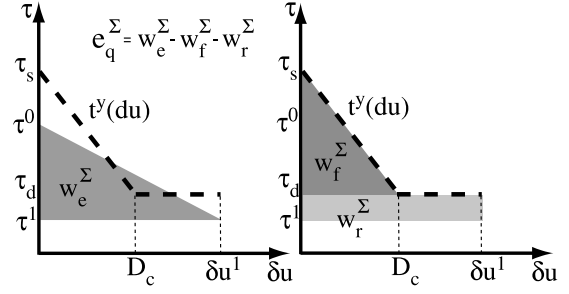


Figure 1. Seismic energy with slip-weakening friction. Each point of the fault provides a seismic energy $e_q^{\Sigma} = w_e^{\Sigma} - w_f^{\Sigma} - w_r^{\Sigma}$. Left: the elastostatic work w_e^{Σ} provided by the elastic crust deformation. Right: the fracture work w_f^{Σ} spent at the rupture front and the relaxation work w_r^{Σ} spent at the arrest. The thick dotted line represents the slip-weakening friction law $\tau^y(\delta u)$.

strongly, up to the P wave velocity locally. This suggests that the pre-stress and the resistance were heterogeneous. From this kinematic model, *Bouchon* [1997] computed the stress history on the fault plane and produced fault maps of static stress drop, $\Delta\tau_{sta}$, dynamic stress drop $\Delta\tau_{dyn}$ and strength excess $\Delta\tau_{exc}$. The initial conditions of our dynamic model are mainly inspired by these maps with some modifications. Our failure criterion does not contain healing and therefore, the final stress τ^1 will be less than but close to the sliding residual stress σ_d . Therefore, to obtain the same static stress drop and slip in our dynamic model as in the kinematic model, we choose our dynamic stress drop equal to the static one computed by *Bouchon* [1997], i.e. $\tau^0 - \sigma_d = \Delta\tau_{sta}$. To define the maximum yield strength σ_s , we just take $\sigma_s = \tau^0 + \Delta\tau_{exc}$ which gives $\sigma_s - \sigma_d = \Delta\tau_{exc} + \Delta\tau_{sta}$. In addition, an unbreakable barrier surrounds the potential slipping domain. These maps of initial conditions are shown in Figure 2.

[8] We use the same vertically layered elastic crust model as *Archuleta* [1984], in which the shear wave velocity is 10 times lower at the surface than at depth. We include the free surface but not the fault dip (20 degrees at most). Since the stratification and the effect of the free surface were not taken into account in the maps produced by *Bouchon* [1997], we found it necessary to decrease the stress drop (and even to make it slightly negative close to the surface) to obtain a reasonable slip at the surface. Finally, due to the unidirectional propagation of the rupture at the hypocenter in the model of *Archuleta* [1984], the stress maps of *Bouchon* [1997] are incompatible with conditions of nucleation. Therefore we modified our dynamic stress drop and strength excess at the hypocenter to produce a more natural nucleation. The single remaining free parameter is the critical slip D_c . For an homogeneous model, we found that $D_c = 0.44$ m is the best value to reproduce the shape of the rupture front velocity found by *Archuleta* [1984]. For smaller D_c the rupture velocity becomes super-shear early, whereas for larger values the rupture stops before breaking the last asperity of the model (see Figure 3).

4. The Computation of the Seismic Energy

4.1. The Fault Mapping, e_q^{Σ}

[9] We have computed the different work densities over the fault w_e^{Σ} , w_f^{Σ} and w_r^{Σ} (see Figure 4). From definition 2,

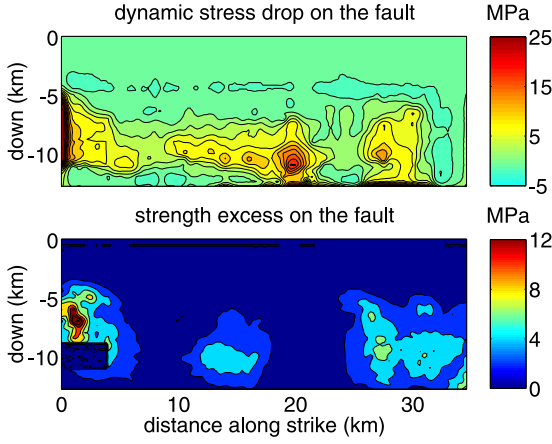


Figure 2. Initial conditions of the dynamic model of the Imperial Valley 1979 earthquake. Contour lines are spaced at 2 MPa. Top: the dynamic stress drop $\tau^0 - \sigma_d$. Bottom: the strength excess $\sigma_s - \tau^0$. These maps are deduced from the stress maps of *Bouchon* [1997] calculated from the kinematic model of *Archuleta* [1984].

the elastostatic work density is related to the product of the final slip and the final stress drop. However, the stress drop is roughly the Hilbert transform of the gradient of the slip, such that the stress can change significantly for small slip variations. Therefore the slip irregularity is fundamental for understanding the source of the seismic energy. The slip-weakening distance being constant and the strength excess moderate, the spent fracture work density is artificially correlated to the stress drop. However, it is natural to think that stronger stress drops are necessary to break stronger barriers of energy; otherwise the rupture would stop. The relaxation work density is very localized on the stronger asperity 20 km from the hypocenter, where the rupture

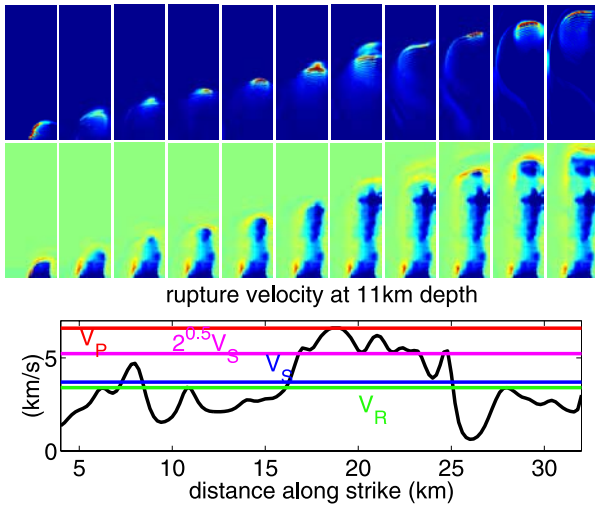


Figure 3. Dynamic model for $D_c = 0.44m$. Top: snapshots of the rupture process on the fault every 0.92s. First panel: the sliding velocity (colorscale 0 to 2 m/s). Second panel: the stress variation (colorscale -10 to 10 MPa). Bottom: the rupture velocity at 11km depth. It is mainly sub-shear (less than V_R), except in the zone 16 to 24km where it is super-shear (between $\sqrt{2}V_S$ and V_P).

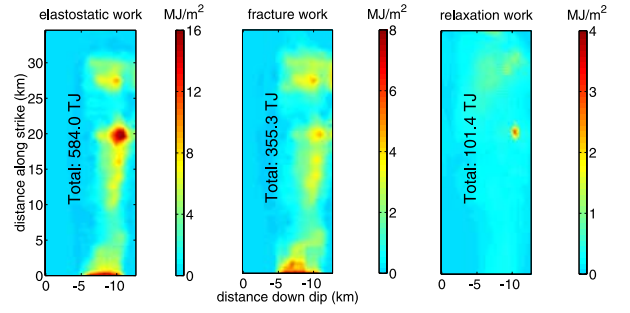


Figure 4. From left to right: the maps of the works densities w_e^Σ , w_f^Σ and w_r^Σ that contribute to the seismic energy. The elastostatic work provides $W_e^\Sigma = 584.0 TJ$. The main loss is due to fracture ($W_f^\Sigma = 355.3 TJ$) at the rupture front, but the relaxation work ($W_r^\Sigma = 101.4 TJ$) at the arrest is not a negligible loss. The resulting total seismic energy is $E_q = W_e^\Sigma - W_f^\Sigma - W_r^\Sigma = 127.3 MJ$.

became supershear. It is a non negligible contribution in the balance of seismic energy.

[10] The resulting seismic energy density $e_q^\Sigma > 0$ is strongly heterogeneous (see the top Figure 5). As shown by the violet contour, it is positive on the main asperities (the source of energy: $e_q^\Sigma > 0$) and negative everywhere else (the sink of energy: $e_q^\Sigma < 0$). In one sense, this energetic picture generalizes the one of *Aki* [1979] on barriers. The reliability of ours is linked to the quality of the initial model: close to the hypocenter it is not well constrained and the rupture stops abruptly without spending energy but in most places it arrests gently in the sinks of energy. We contour in black the smallest possible area that can account for the radiated energy E_q (the excess zone of energy); outside this excess zone, the integral of the energy density is zero. Compared to the final slip distribution (at bottom of Figure 5), which shows that the fault has ruptured everywhere, the source and the excess zone of energy are very small portions of the

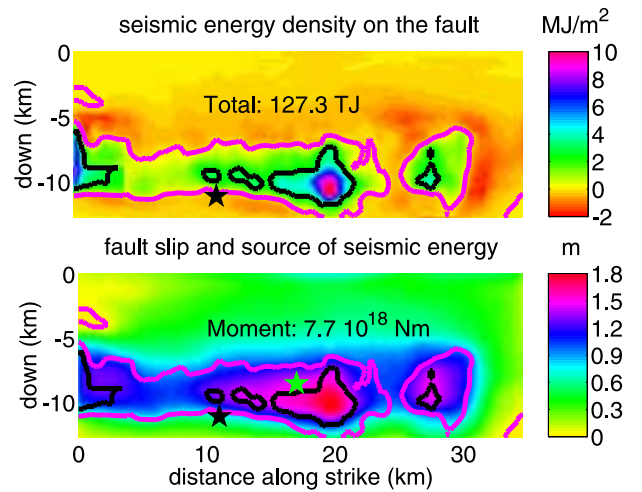


Figure 5. Dynamic and static fault representations. Top: the seismic energy density e_q^Σ and its centroid (black star). Outside the violet contour we have $e_q^\Sigma < 0$. Outside the black contour the net seismic energy is null and inside we have the concentrated excess of energy, i.e. E_q . Bottom: the map of the final slip δu^1 , the moment centroid (green star) and the contours related to seismic energy.

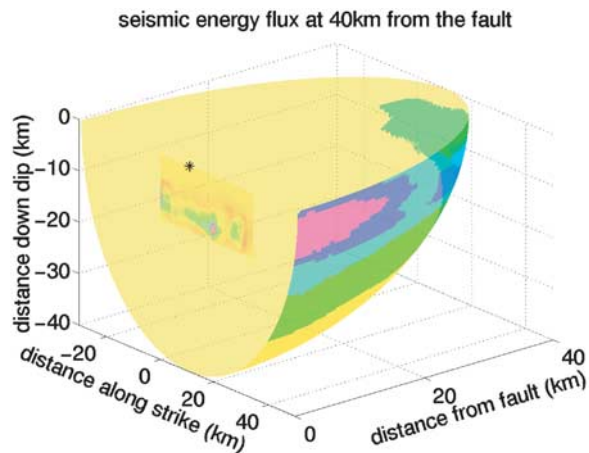


Figure 6. Combined Representation of source (fault mapping) and directivity (distant mapping). On the hemisphere S of radius $R = 40\text{km}$, centered above the centroid of seismic energy (black star), we represent the seismic energy flux e_q^S (only on one quarter by symmetry). Each color on S corresponds to the generation of 20% of E_q , at different intensities (decreasing from red to yellow, via dark blue, light blue and green). 40% of the energy passes through 6.4% of the sphere (red and dark blue).

ruptured fault. We conjecture that, these zones should have an observable signature in the radiation of the source.

4.2. The Distant Mapping, e_q^S

[11] Here, our goal is to characterize the flux of seismic energy release in the near-field and to test the energy balance (1) in the finite-difference dynamic modeling. For this, we used a large finite difference grid and defined S as the surface of three hemispheres of radius $R = 30, 35$ and 40 km. These hemispheres are centered on the surface above the centroid of seismic energy, and closed by the free surface (for which energy flux is impossible by definition).

[12] We computed the density $e_q^S = w_q^S - w_e^S$, simultaneously with the rupture (see Figure 6). To ensure the complete escape of the energy through S with direct, reflected and surface waves, the final time $t^1 = 93\text{s}$. For the three values of R , we found $W_q^S - W_e^S = 124.5\text{ TJ}$. That is consistent with $W_q^S - W_e^S = E_q = W_e^\Sigma - W_f^\Sigma - W_r^\Sigma$ at about 1.1% of accuracy. For $R = 30$ km and 40 km we have respectively $W_e^S/E_q = 9.06\%$ and $W_e^S/E_q = 3.26\%$, which indicates that these hemispheres are not in the far-field, and the work done by the static field must be taken into account to balance the energy. The directivity is very strong because 86% of the energy is emitted in the forward direction. Also 40% of the energy passes through 6.4% of the sphere. The energy is confined between 5 and 15 km depth and with little energy traveling in the upper layers because of their low shear modulus.

5. Conclusion

[13] We have presented a mechanical approach to the analysis of seismic energy released by a fault rupture. The

use of a dynamic model, with a constitutive slip-weakening friction law, allows us to show clearly the contribution of the slip, the stress drop, the rupture propagation and its arrest. For our model of the 1979 Imperial Valley earthquake, which contains asperities and barriers, we find that a large part of the fault is a sink of energy while a relatively smaller area is the *source*, in which an even smaller part concentrates the positive residue E_q , the *excess zone*. We have computed the seismic energy that passes across three hemispheres enclosing the Imperial Fault and its very heterogeneous vertical crustal structure. We have included the bias induced by the elastostatic field in the near field and we have verified the energies balance successfully. The flux of seismic energy across these hemispheres produce a global map of directivity. In term of energy the directivity is spectacular; moreover the source radiates in a very small angular aperture in the forward direction.

[14] **Acknowledgments.** We are very grateful to S. Nielsen and an anonymous reviewer for their review of the manuscript. We want to thank Michel Bouchon for his comments and his assistance in providing the stress maps that are necessary for this work. This project was supported by the W. M. Keck Foundation grant to UCSB for an Interdisciplinary Program in Materials Physics and Seismology. This research was supported by the Southern California Earthquake Center. SCEC is funded by NSF Cooperative Agreement EAR-8920136 and USGS Cooperative Agreements 14-08-0001-A0899 and 1434-HQ-97AG01718. The SCEC contribution number for this paper is 692. RJA would also acknowledge the CNRS for its support during three months spent at the LGIT, Observatoire de Grenoble, Université Joseph Fourier, Grenoble, where this project was launched. Part of the computations presented in this paper were performed at the Service Commun de Calcul Intensif de l'Observatoire de Grenoble (SCCI). This is ICS Contribution No 552.

References

- Aki, K., Generation of G-waves from the Niigata earthquake of June 16, 1964, 2, Estimation of earthquake movement, released energy and stress-strain drop from G-wave spectrum, *Bull. Earthquake Res. Inst. Univ. Tokyo*, 44, 23–88, 1966.
- Aki, K., Characteristics of barriers on an earthquake fault, *J. Geophys. Res.*, 84, 6140–6148, 1979.
- Andrews, D. J., Test of two methods for faulting in finite-difference calculation, *Bull. Seismol. Soc. Am.*, 89, 931–937, 1999.
- Archuleta, R., A faulting model for the 1979 Imperial Valley earthquake, *J. Geophys. Res.*, 89, 4559–4585, 1984.
- Bouchon, M., The state of stress of some faults of the San Andreas system as inferred from near-field strong motion data, *J. Geophys. Res.*, 102, 11,731–11,744, 1997.
- Choy, G. L., and J. Boatwright, Global patterns of radiated seismic energy and apparent stress, *J. Geophys. Res.*, 100, 18,205–18,228, 1995.
- Gutenberg, B., and C. F. Richter, Earthquake magnitude, intensity, and acceleration, *Bull. Seismol. Soc. Am.*, 3, 163–191, 1942.
- Kanamori, H., J. Mori, E. Hauksson, T. H. Heaton, L. K. Hutton, and L. Jones, Determination of earthquake energy release and M_L using TERRAscope, *Bull. Seismol. Soc. Am.*, 83, 330–346, 1993.
- Kostrov, B. V., Seismic moment and energy of earthquakes and seismic flow of rock, *Izv. Earth Phys.*, 1, 23–40, 1974.
- Madariaga, R., Dynamics of an expanding circular crack, *Bull. Seismol. Soc. Am.*, 3, 639–666, 1976.
- Moczo, P., J. Kristek, R. Archuleta, and L. Halada, 3D staggered-grid finite-difference modeling with volume harmonic and arithmetic averaging of elastic moduli and densities, *Bull. Seismol. Soc. Am.*, in press, 2003.
- Peyrat, S., K. B. Olsen, and R. Madariaga, Dynamic modeling of the 1992 Landers earthquake, *J. Geophys. Res.*, 106, 26,467–26,482, 2001.

P. Favreau and R. J. Archuleta, Institute for Crustal Studies, University of California at Santa Barbara, CA 93106, USA. (pfavre@crustal.ucsb.edu; ralph@crustal.ucsb.edu)